Journal of Electroceramics 3:4, 347–359, 1999


# A Large Piezoelectric Anisotropy of a Three-Component Composite with Variable Connectivity

VITALI YU TOPOLOV[1,2] & ANATOLY V. TURIK[2]

[1]*Institut für Werkstoffe der Elektrotechnik II, Rheinisch-Westfälische Technische Hochschule Aachen, Templergraben 55, D-52056 Aachen, Germany*

[2]*Department of Physics, Rostov State University, Zorge str. 5, 344090 Rostov-on-Don, Russia*

Submitted December 15, 1998; Revised February 25, 1999; Accepted April 15, 1999

**Abstract.** Proposed are two types of three-component piezoelectric composites that change connectivity from 2-2 to 1-3 and contain polarized ferroelectric ceramic and polymer components, i.e., ''layer 1 reinforced by rods–layer 2–layer 1 reinforced by rods– . . . '' (type 1) and ''laminated rods (layer 1–layer 2–layer 1– . . . ) embedded in a matrix'' (type 2). Some cases of the large anisotropy of piezoelectric coefficients $d_{33}^*/|d_{31}^*|$ and $e_{33}^*/|e_{31}^*|$ are analyzed for the composites of the type 1. Original cases of simultaneous reaching $d_{33}^*/|d_{31}^*| \to 0$ and $e_{33}^*/|e_{31}^*| > 10$ as well as $e_{33}^*/|e_{31}^*| \to \infty$ and $d_{33}^*/|d_{31}^*| \to \infty$ at different volume concentrations of the components in the composites of the type 2 are also considered. It is shown that these ratios essentially depend on electromechanical constants of the components, their volume concentrations, microgeometry, as well as on jumps of these constants and internal fields at boundaries between the components.

**Keywords:** composites, electromechanical properties, perovskite ferroelectric ceramics, large piezoelectric anisotropy

## 1. Introduction

An interest in the problem of the large piezoelectric anisotropy in ferroelectrics and related materials [1] is associated with studying different physical phenomena and with various applications of these materials. An attractive group of such the materials can be found among piezoactive composites [2-4] having different components, connectivity (microgeometry), etc. The problems of modeling of composite structures [5,6], the optimization and anisotropy of their electromechanical properties are difficult and associated with taking into account many physical, chemical, technological, and other factors.

A considerable part of publications deals with theoretical prognostications and evaluations of effective electromechanical properties of two-component piezoactive composites with concrete connectivity, e.g., 2–2 (laminates) [7], 1–3 (fibrous structures) [8–11], 0–3 (inclusions within a matrix) [11–14], etc. These properties are determined by using analytical methods, which are often based on the effective medium theory [11,12] or the matrix representation [13,14] of an anisotropic electroelastic behavior of constituent materials, or on a finite element analysis [5,15,16]. This analysis is connected with various configurations and arrangement of inclusions embedded in a matrix as well as with the optimization of the composite properties. Both the analytical and finite element methods are characterized by taking into account boundary conditions for elastic and electric fields (i.e., mechanical strain (stress) and electric strength (displacement) components), and these conditions directly influence basic physical properties of the composites with different connectivity.

As a rule, the above-mentioned and related methods are applied to different two-component composites, and it seems to be interesting to extend further evaluations at some multicomponent composite structures. The present work is devoted to a theoretical substantiation of a possibility for creating

three-component composites which contain polarized ferroelectric ceramics (PFC) and polymers and show the variable anisotropy of piezoelectric charge coefficients $d^*_{3j}$ and the sufficiently large anisotropy of piezoelectric strain coefficients $e^*_{3j}$. For a comparison and better understanding of reasons for the considerable piezoelectric anisotropy we consider two alternative composite structures changing their connectivity from 2–2 to 1–3 and vice versa.

## 2. Structures of Composites and Basic Formulas

The composite of the type 1 (Fig. 1(a)) contains two-component layers 1 and one-component layers 2 [2]. The layer 1 is described as a polymer matrix with a system of long PFC rods or prolate spheroidal inclusions oriented and polarized along the $OX_3$ axis of a rectangular $(X_1X_2X_3)$ coordinate system. The layer 2 can contain only one PFC or polymer component polarized along the same axis. The layers 1 and 2 alternate along the $OX_3$ axis, and interfaces between them are assumed to be parallel to the $(X_1OX_2)$ plane. The composite of the type 2 (Fig. 1(b)) consists of a system of the laminated two-component (ceramic, polymer) rods embedded in the polymer matrix. As in the case of the type 1, the rods are oriented and polarized along the $OX_3$ axis, the matrix is also polarized along the same axis, and the layers 1 and 2 are separated by the interfaces being parallel to the $(X_1OX_2)$ plane.

Elastic, dielectric, and piezoelectric properties of the above-described composites of types 1 and 2 are determined by using formulas for the laminated and fibrous two-component piezoactive composites. These formulas are results of averaging the electromechanical constants of the constituent materials by taking into account boundary conditions at planar or circular interfaces. For example, such the conditions for the layers interfaces $x_3 = \text{const}$ in the 2–2 composite suppose continuity of mechanical stress $\sigma_{13}$, $\sigma_{23}$, $\sigma_{33}$ and strain $\xi_{11}$, $\xi_{12}$, $\xi_{22}$ components as well as electric strength $E_1$, $E_2$ and displacement $D_3$ components. For 1–3 connectivity additionally one can introduce a cylindrical coordinate $(r, \theta, z)$ system connected with a rod of the composite, where $r$ and $\theta$ are radial and angle coordinates on the $(X_1OX_2)$ plane, respectively, and the $z$ axis coincides with the $OX_3$ axis shown in Fig. 1. Corresponding conditions to be satisfied at a boundary between the rod and the matrix are associated with coninuous mechanical displacement $u_r$, $u_z$ and stress $\sigma_{rz}$ components as well as electric strength $E_\theta$ and displacement $D_r$ components.

Averaged elastic $c^E_{fg,l}$ and piezoelectric $e_{3j,l}$ constants of the 2–2 composite [3,17], which are used for further calculations of $d^*_{3j}$ and $e^*_{3j}$ of our composites of both the types, are written below:

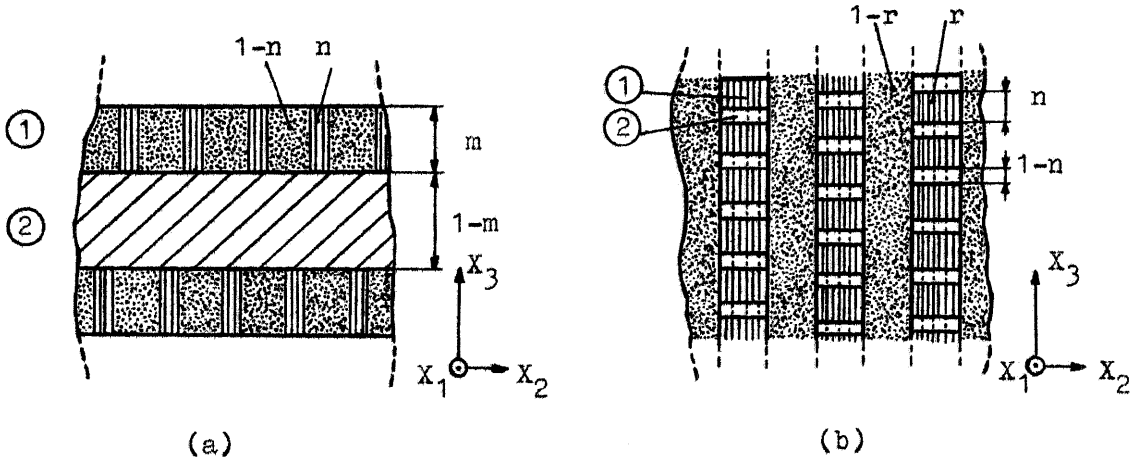


*Fig. 1.* Cross-sections of two proposed composite structures by the $(X_2OX_3)$ plane.
(a), $m$ and $1-m$ are volume concentrations of layers 1 and 2 respectively, $n$ and $1-n$ are volume concentrations of rods and a matrix surrounding these rods in the layer 1, respectively; (b), $n$ and $1-n$ are volume concentrations of layers 1 and 2, respectively, being constituent parts of rods, $r$ and $1-r$ are volume concentrations of these laminated rods and the surrounding matrix, respectively.
The electrical poling direction coincides with the $(OX_3)$ direction.

$$
\left.\begin{aligned}
c^E_{11,l} &= c^{(1),E}_{11}m_1 + c^{(2),E}_{11}m_2 - (m_1m_2/\Delta)[(c^{(1),E}_{13} - c^{(2),E}_{13})^2(\chi^{(2),\xi}_{33}m_1 + \chi^{(1),\xi}_{33}m_2) \\
&\quad + 2(c^{(1),E}_{13} - c^{(2),E}_{13})(e^{(1)}_{31} - e^{(2)}_{31})(e^{(2)}_{33}m_1 + e^{(1)}_{33}m_2) - (e^{(1)}_{31} - e^{(2)}_{31})^2(c^{(2),E}_{33}m_1 + c^{(1),E}_{33}m_2)], \\
c^E_{12,l} &= c^{(1),E}_{12}m_1 + c^{(2),E}_{12}m_2 - (m_1m_2/\Delta)[(c^{(1),E}_{13} - c^{(2),E}_{13})^2(\chi^{(2),\xi}_{33}m_1 + \chi^{(1),\xi}_{33}m_2) \\
&\quad + 2(c^{(1),E}_{13} - c^{(2),E}_{13})(e^{(1)}_{31} - e^{(2)}_{31})(e^{(2)}_{33}m_1 + e^{(1)}_{33}m_2) - (e^{(1)}_{31} - e^{(2)}_{31})^2(c^{(2),E}_{33}m_1 + c^{(1),E}_{33}m_2)], \\
c^E_{13,l} &= c^{(1),E}_{13}m_1 + c^{(2),E}_{13}m_2 - (m_1m_2/\Delta)\{(c^{(1),E}_{13} - c^{(2),E}_{13})[(c^{(1),E}_{33} - c^{(2),E}_{33}) \\
&\quad \times (\chi^{(2),\xi}_{33}m_1 + \chi^{(1),\xi}_{33}m_2) + (e^{(1)}_{33} - e^{(2)}_{33})(e^{(2)}_{33}m_1 + e^{(1)}_{33}m_2)] - (e^{(1)}_{31} - e^{(2)}_{31}) \\
&\quad \times [(e^{(1)}_{33} - e^{(2)}_{33})(c^{(2),E}_{33}m_1 + c^{(1),E}_{33}m_2) - (c^{(1),E}_{33} - c^{(2),E}_{33})(e^{(2)}_{33}m_1 + e^{(1)}_{33}m_2)]\}, \\
c^E_{33,l} &= c^{(1),E}_{33}m_1 + c^{(2),E}_{33}m_2 - (m_1m_2/\Delta)[(c^{(1),E}_{33} - c^{(2),E}_{33})^2(\chi^{(2),\xi}_{33}m_1 + \chi^{(1),\xi}_{33}m_2) \\
&\quad + 2(c^{(1),E}_{33} - c^{(2),E}_{33})(e^{(1)}_{33} - e^{(2)}_{33})(e^{(2)}_{33}m_1 + e^{(1)}_{33}m_2) - (e^{(1)}_{33} - e^{(2)}_{33})^2(c^{(2),E}_{33}m_1 + c^{(1),E}_{33}m_2)], \\
e_{31,l} &= e^{(1)}_{31}m_1 + e^{(2)}_{31}m_2 - (m_1m_2/\Delta)\{(e^{(1)}_{33} - e^{(2)}_{33})[(c^{(1),E}_{13} - c^{(2),E}_{13}) \\
&\quad \times (\chi^{(2),\xi}_{33}m_1 + \chi^{(1),\xi}_{33}m_2) + (e^{(1)}_{31} - e^{(2)}_{31})(e^{(2)}_{33}m_1 + e^{(1)}_{33}m_2) + (\chi^{(1),\xi}_{33} - \chi^{(2),\xi}_{33}) \\
&\quad \times [(e^{(1)}_{31} - e^{(2)}_{31})(c^{(2),E}_{33}m_1 + c^{(1),E}_{33}m_2) - (c^{(1),E}_{13} - c^{(2),E}_{13})(e^{(2)}_{33}m_1 + e^{(1)}_{33}m_2)]\},
\end{aligned}\right\} \tag{1}
$$

and

$$
\left.\begin{aligned}
e_{33,l} &= e^{(1)}_{33}m_1 + e^{(2)}_{33}m_2 - (m_1m_2/\Delta)\{(e^{(1)}_{33} - e^{(2)}_{33})[(c^{(1),E}_{33} - c^{(2),E}_{33})(\chi^{(2),\xi}_{33}m_1 \\
&\quad + \chi^{(1),\xi}_{33}m_2) + (e^{(1)}_{33} - e^{(2)}_{33})(e^{(2)}_{33}m_1 + e^{(1)}_{33}m_2)] + (\chi^{(1),\xi}_{33} - \chi^{(2),\xi}_{33})[(e^{(1)}_{33} \\
&\quad - e^{2}_{33})(c^{(2),E}_{33}m_1 + c^{(1),E}_{33}m_2) - (c^{(1),E}_{33} - c^{(2),E}_{33})(e^{(2)}_{33}m_1 + e^{(1)}_{33}m_2)]\}
\end{aligned}\right\}
$$

where $m_k$, $c^{(k),E}_{fg}$, $e^{(k)}_{ij}$, and $\chi^{(k),\xi}_{pp}$ are the volume concentration, elastic, piezoelectric, and dielectric constants of the $k$th component (layer), respectively, $k = 1; 2$, $m_2 = 1 - m_1$, and

$$
\begin{aligned}
\Delta &= (c^{(2),E}_{33}m_1 + c^{(1),E}_{33}m_2)(\chi^{(2),\xi}_{33}m_1 + \chi^{(1),\xi}_{33}m_2) \\
&\quad + (e^{(2)}_{33}m_1 + e^{(1)}_{33}m_2)^2
\end{aligned}
$$

In accordance with results [10] averaged piezoelectric constants of the 1–3 composite are expressed in a form

$$
\left.\begin{aligned}
d_{31,r} &= \{[2d^{(1)}_{31}s^{(2),E}_{11}r + d^{(2)}_{31}(s^{(1),E}_{11} + s^{(1),E}_{12} + s^{(2),E}_{11} - s^{(2),E}_{12})(1 - r)][s^{(2),E}_{33}r \\
&\quad + s^{(1),E}_{33}(1 - r)] - 2[s^{(2),E}_{13}r + s^{(1),E}_{13}(1 - r)][d^{(1)}_{31}s^{(2),E}_{13}r + d^{(2)}_{31}s^{(1),E}_{13}(1 - r)] \\
&\quad + (d^{(1)}_{33} - d^{(2)}_{33})[(s^{(1),E}_{11} + s^{(1),E}_{12} + s^{(2),E}_{11} - s^{(2),E}_{12})s^{(2),E}_{13} - 2s^{(2),E}_{11}s^{(1),E}_{13}]r(1 - r)\}A^{-1}, \\
d_{33,r} &= \{[(s^{(2),E}_{11} + s^{(2),E}_{12})r + (s^{(1),E}_{11} + s^{(1),E}_{12})(1 - r) + s^{(2),E}_{11} \\
&\quad - s^{(2),E}_{12}][d^{(1)}_{33}s^{(2),E}_{33}r + d^{(2)}_{33}s^{(1),E}_{33}(1 - r)] - 2[s^{(2),E}_{13}r + s^{(1),E}_{13}(1 - r)][d^{(1)}_{33}s^{(2),E}_{13}r \\
&\quad + d^{(2)}_{33}s^{(1),E}_{13}(1 - r)] + 2(d^{(1)}_{31} - d^{(2)}_{31})(s^{(1),E}_{33}s^{(2),E}_{13} - s^{(2),E}_{33}s^{(1),E}_{13})r(1 - r)\}A^{-1}, \\
e_{31,r} &= [2e^{(1)}_{31}c^{(2),E}_{11}r + e^{(2)}_{31}(c^{(1),E}_{11} + c^{(1),E}_{12} + c^{(2),E}_{11} - c^{(2),E}_{12})(1 - r)]C^{-1},
\end{aligned}\right\} \tag{2}
$$

and

$$
\left.\begin{aligned}
e_{33,r} &= e^{(1)}_{33}r + e^{(2)}_{33}(1 - r) - 2r(1 - r)(e^{(1)}_{31} - e^{(2)}_{31})(c^{(1),E}_{13} - c^{(2),E}_{13})C^{-1}
\end{aligned}\right\}
$$

where $r$ is the volume concentration of the rods $(k = 1)$, $c_{fg}^{(k),E}$ and $s_{fg}^{(k),E}$ are elastic moduli and compliances, respectively, $e_{3j}^{(k)}$ and $s_{3j}^{(k)}$ are piezoelectric constants, and $k = 2$ corresponds to the matrix. The $A$ and $C$ factors introduced in Eqs. (2) are determined as

$$A = [(s_{11}^{(2),E} + s_{12}^{(2),E})r + (s_{11}^{(1),E} + s_{12}^{(1),E})(1-r) + s_{11}^{(2),E} - s_{12}^{(2),E}][s_{33}^{(2),E}r + s_{33}^{(1),E}(1-r)] - 2[s_{13}^{(2),E}r + s_{13}^{(1),E}(1-r)]^2$$

and

$$C = c_{11}^{(2),E} - c_{12}^{(2),E} + (c_{11}^{(2),E} + c_{12}^{(2),E})r + (c_{11}^{(1),E} + c_{12}^{(1),E})(1-r)$$

All the expressions listed in Eqs. (1) and (2) have been derived for the composites polarized along the $OX_3$ axis and characterized [3] by a transversal isotropy ($\infty mm$).

In next sections of this paper we consider some examples of the piezoelectric coefficients $e_{3j}^*(m,n)$ and $d_{3j}^*(m,n)$ (type 1, $j = 1;3$) or $e_{3j}^*(n,r)$ and $d_{3j}^*(n,r)$ (type 2, $j = 1;3$) as well as their anisotropy $\zeta_e^* = e_{33}^*/e_{31}^*$ and $\zeta_d^* = d_{33}^*/d_{31}^*$. For the type 2 we introduce dimensionless functions $e_{3j}^*(m,r)/e$ and $d_{3j}^*(m,r)c/e$, where $e = e_{33}^{(M)}$ and $c = c_{33}^{(M),E}$ are the piezoelectric strain coefficient and the elastic modulus of the matrix in the $OX_3$ direction, respectively. The above-mentioned volume concentrations $m$, $n$, and $r$ of different components are determined as shown in Fig. 1.

## 3. Piezoelectric Coefficients $e_{3j}^*$ and $d_{3j}^*$

Piezoactive materials, which can be used as components, are distinguished (Table 1) by signs and ratios of the piezoelectric strain coefficients $e_{3j}^{(k)}(j = 1;3)$, and these factors strongly influence the calculated concentration dependences of the piezoelectric properties. In order to avoid taking into account an additional effect of considerable internal mechanical stresses, appearing in vicinities of ends of the rods (type 1, see Fig. 1(a)) or between the matrix and layers interfaces (type 2, see Fig. 1(b)), one can consider, e.g., a region of their sufficiently small volume concentrations $0 < n \leq 0.25$ for the type 1 or a region of the concentrations $0.75 \leq n < 1$ showing a prevalence of the layers 1 in comparison with the layers 2 for the type 2. Various examples of the concentration behavior of the composite piezoelectric coefficients $e_{3j}^*(m,n)$ and $d_{3j}^*(m,n)$ (type 1) or $e_{3j}^*(n,r)/e$ and $d_{3j}^*(n,r)c/e$ (type 2) are plotted in Figs. 2–6. The $e_{31}^*(m,n)$ and $d_{31}^*(m,n)$ functions determined for the type 1 undergo appreciable variations at changing both the $m$ and $n$ concentrations and/or at choosing piezoactive components with various $e_{33}^{(k)}/e_{31}^{(k)}$ ratios. All the calculated $e_{3j}^*(m,n)$ and $d_{3j}^*(m,n)$ functions can be nonmonotonic within the above-mentioned concentration ranges, and many extreme are reached for small $n$ values, as shown, for example, in Figs. 3(a–f) and 4(a, b). A reason for such the behavior is associated with a presence of the modified $PbTiO_3$ PFC or the VDF/TrFE: both these components are characterized by unusual signs of $e_{3j}^{(k)}$ (see Table 1), that give rise to an original distribution of electric and elastic fileds within samples and enables to change the signs of the effective piezoelectric coefficients $e_{3j}^*(m,n)$ of the composite as a whole (see, e.g., Figs. 2(a, b), 3(f), and 4(a, b)).

As follows from our further calculations, the presence of the non-piezoelectric araldite [4] matrix within the layer 1 does not lead to significant changes in the concentration dependences of the piezoelectric properties of the composite of the type 1. This and other results testify to the main role of the PFC components in forming and changing the piezoelectric anisotropy of the composite of the type 1.

One of the reasons for the various $e_{3j}^*(m,n)$ functions determined for the type 1 consists in a

*Table 1*. Experimental values of piezoelectric strain coefficients $e_{3j}^{(k)}$ of different PFC and polymer components at room temperature

| Components | PZT-4 PFC, [3,18] | ZTS-19 PFC (PZT-type), [3] | Modified $PbTiO_3$ PFC, [18] | (Ba,Ca,Pb)$TiO_3$ PFC, [3,18] | (Pb,Ba) ($Zr,TiO_3$), [3,18] | VDF polymer, [3,18] | 75/25 mol. % copolymer of $VF_2$ and TrFE(VDF /TrFE), [8] |
|---|---|---|---|---|---|---|---|
| $e_{3j}^{(k)}$, C/m$^2$ | − 5.2 | − 4.9 | 0.458 | − 0.68 | − 7.9 | − 1.1 | 0.008 |
| $e_{33}^{(k)}$, C/m$^2$ | 15.1 | 14.9 | 6.50 | 7.71 | 17.7 | 2.9 | − 0.29 |

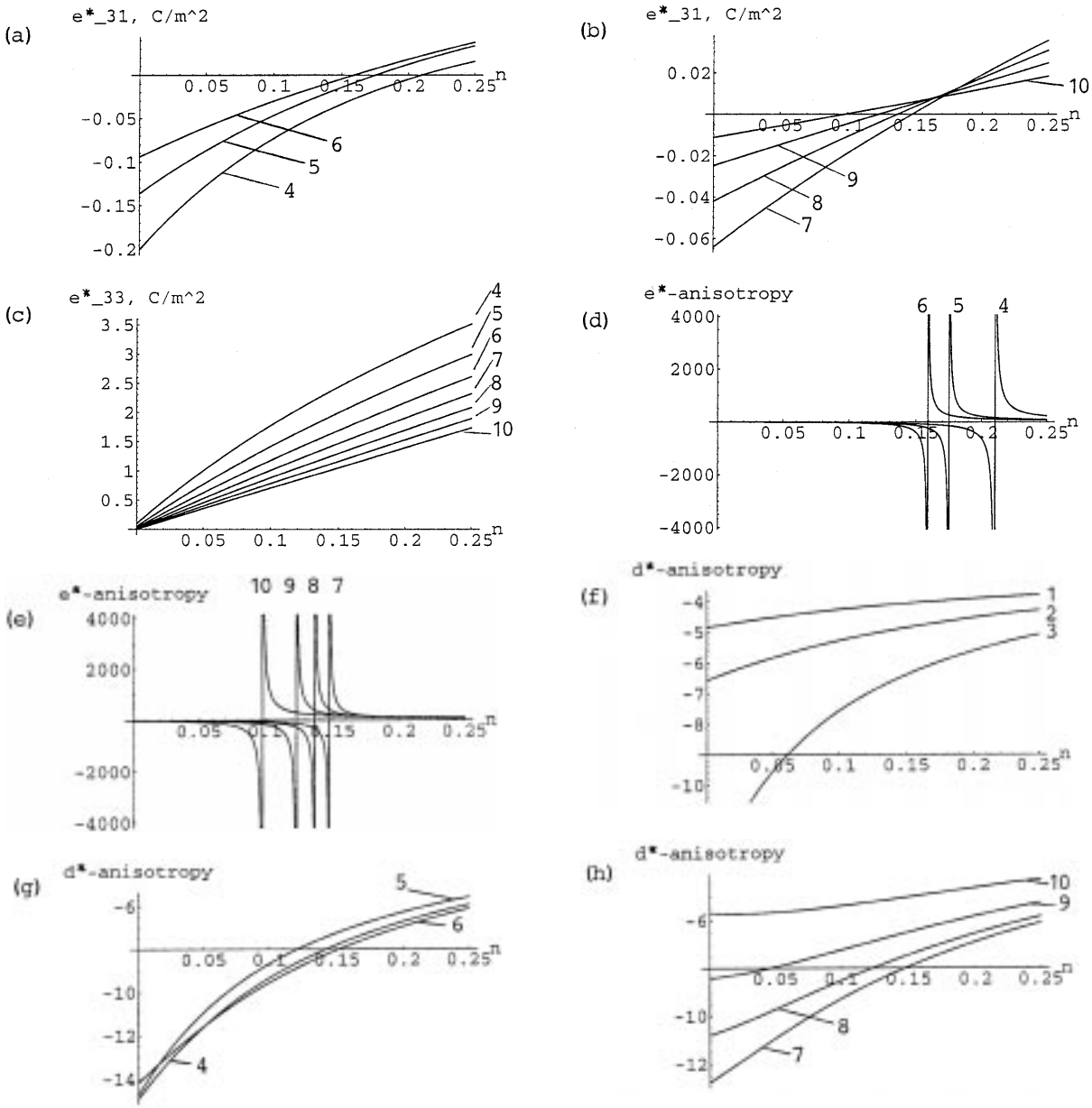


*Fig. 2.* Concentration dependences of the piezoelectric properties calculated for the composite of the type 1 (layers 1: modified $PbTiO_3$ PFC rods + VDF matrix, layers 2: (Ba, Ca, Pb)$TiO_3$ PFC). (a) and (b), $e^*_{31}(m,n)$ for fixed $m$ values; (c), $e^*_{33}(m,n)$ for fixed $m$ values; (d) and (e), $\zeta^*_e(m,n)$ for fixed $m$ values; (f), (g), and (h), $\zeta^*_d(m,n)$ for fixed $m$ values; In all the plots, marking figures 1, 2, 3, 4, 5, 6, 7, 8, 9, and 10 correspond to volume concentrations $m = 0.01$, 0.1, 0.2, 0.3, 0.4, 0.5, 0.6, 0.7, 0.8, and 0.9, respectively.

feature of a distribution of internal elastic and electric fields within the composite sample: the piezoactive rods are embedded in the matrix (see Fig. 1(a)) with a low or zero piezoelectric activity, that impedes the piezoelectric interaction but does not prevent a redistribution of internal stress fields along the $OX_1$ and $OX_2$ axes. Both the layers 1 and 2 as a whole remain their piezoelectric activity and, therefore, the piezoelectric interaction along the $OX_3$ axis. This circumstance as well as differences in elastic properties of the components [4,8,18] of the layers 1 and 2 can influence the piezoelectric coefficient $e^*_{31}$ that

reflects the electromechanical interactions along the $OX_1$ and $OX_3$ axes being non-polar and polar directions for the composite sample, respectively. In contrast to the $e^*_{31}(m,n)$ functions, the $e^*_{33}(m,n)$ ones correspond to the electromechanical interaction along the $OX_3$ direction without a considerable influence of differences in elastic and dielectric properties of the mentioned layers.

A considerable feature of the $e^*_{3j}(n,r)$ and $d^*_{3j}(n,r)$ plots at $n \to 1$ for the type 2 consists in a sufficiently slight dependence of these functions on the $n$ concentration in a case of the VDF matrix (Fig. 5(a,b)) and in their distinct dependence on $n$ in a case of the VDF/TrFE matrix (Fig. 6(a–f)) that can be interpreted by different $sgne^{(k)}_{3j}$ of the components (see Table 1). So, the plots in Fig. 5(a,b) are typical of the situation when all the constants $e^{(k)}_{33} > 0$, and the volume concentration $n$ reflecting a distribution of the

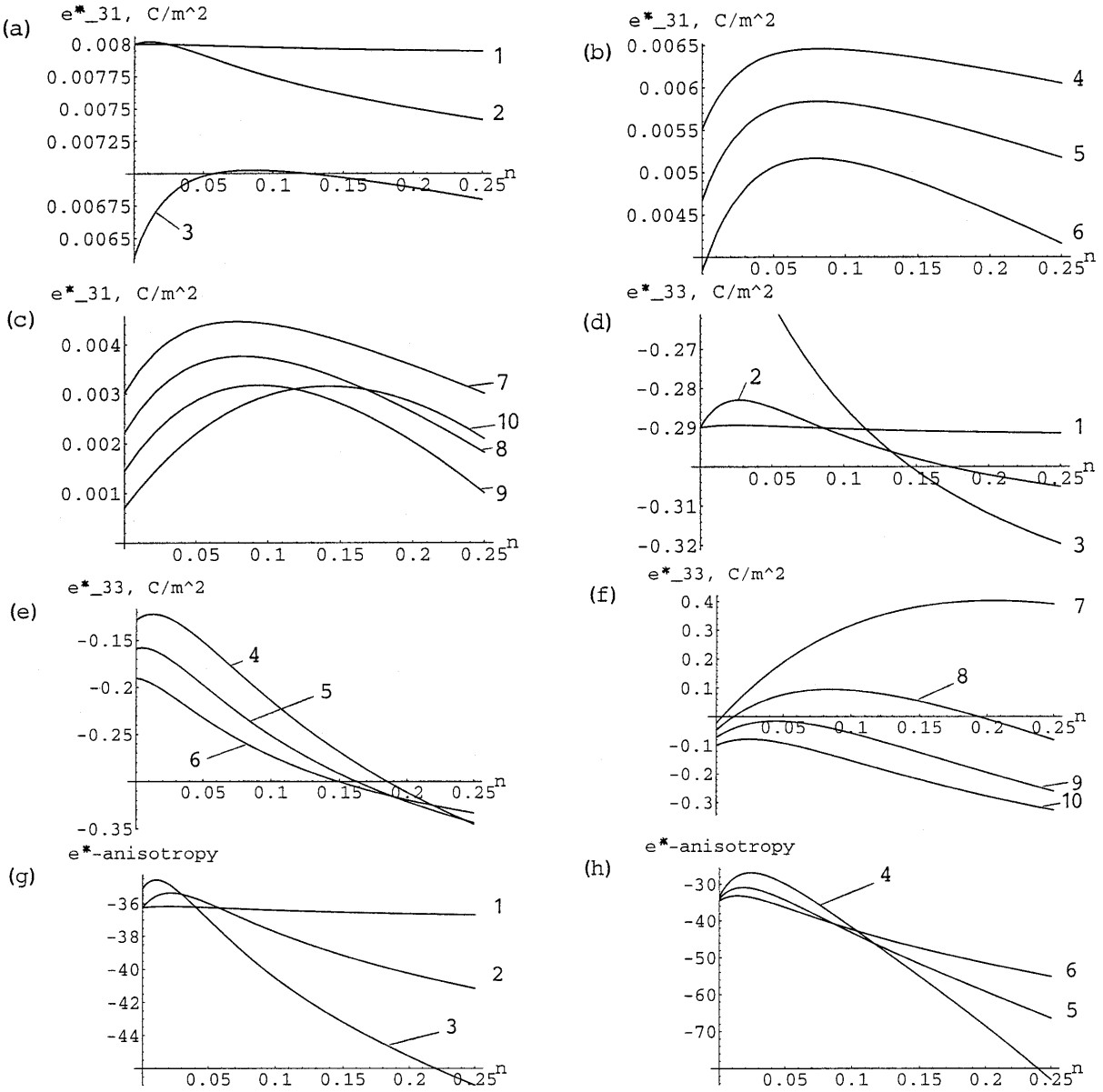


*Fig. 3.* Concentration dependences of the piezoelectric properties calculated for the composite of the type 1 (layers 1: modified $PbTiO_3$ PFC rods + VDF/TrFE matrix, layers 2: VDF/TrFE). (a), (b), and (c), $e^*_{31}(m,n)$ for fixed $m$ values; (d), (e), and (f), $e^*_{33}(m,n)$ for fixed $m$ values; (g), (h), and (i), $\zeta^*_e(m,n)$ for fixed $m$ values; (j), $d^*_{31}(m,n)$ for fixed $m$ values; (k), $d^*_{33}(m,n)$ for fixed $m$ values. In all the plots, marking figures 1, 2, 3, 4, 5, 6, 7, 8, 9, and 10 correspond to volume concentrations $m = 0.01$, 0.1, 0.2, 0.3, 0.4, 0.5, 0.6, 0.7, 0.8, and 0.9, respectively.

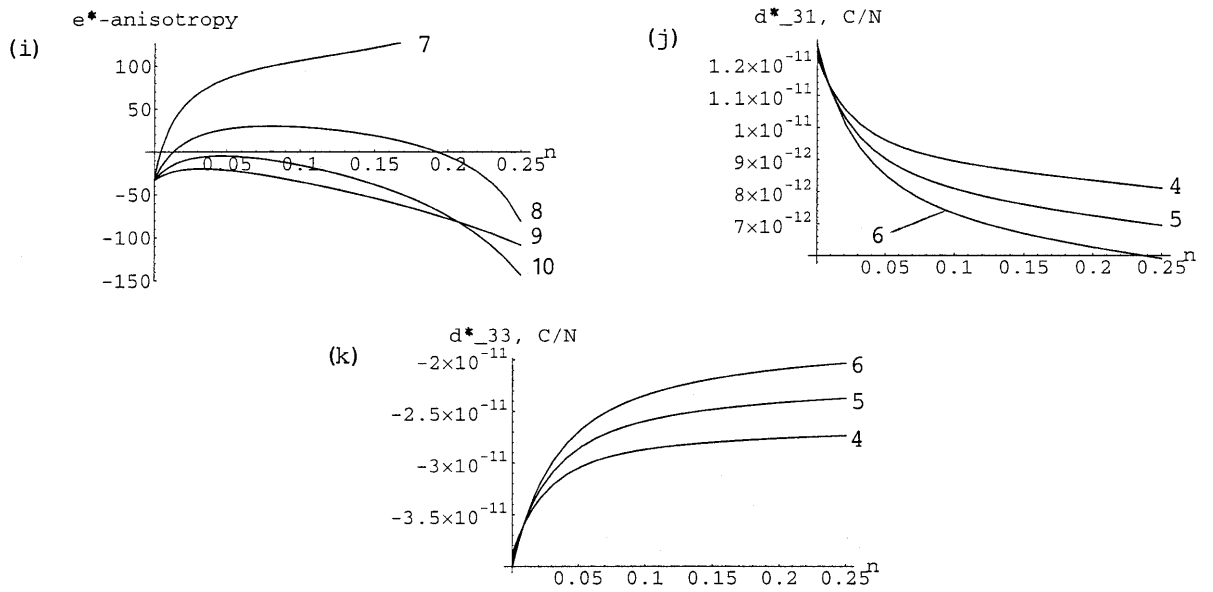


*Fig. 3.* (*Continued*)

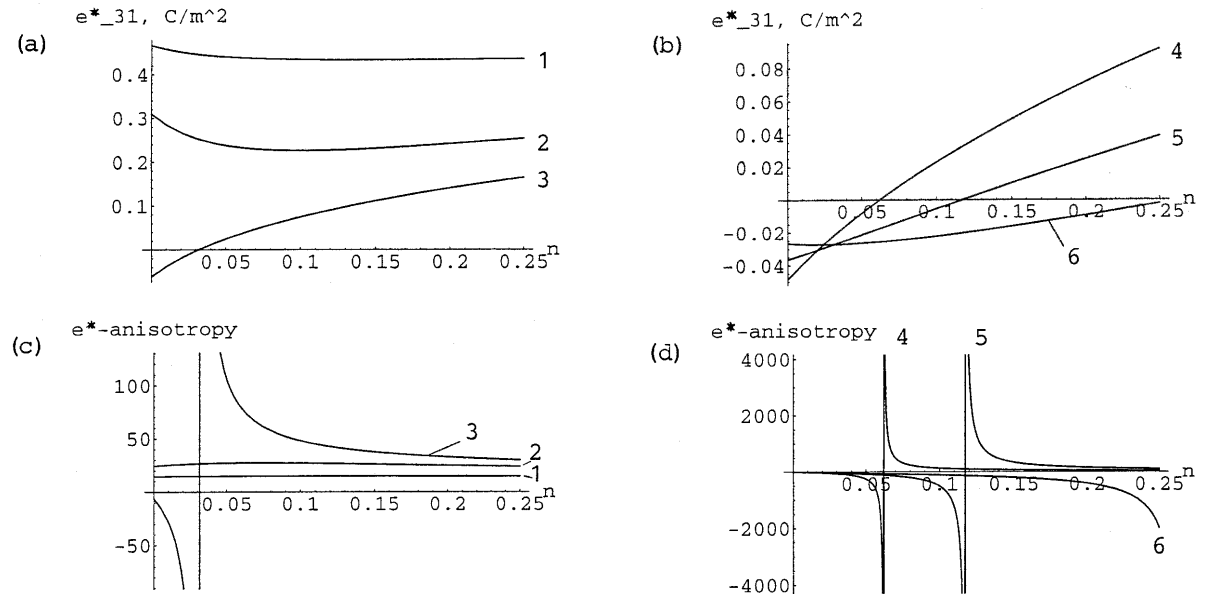


*Fig. 4.* Concentration dependences of the piezoelectric properties calculated for the composite of the type 1 (layers 1: ZTS-19 PFC rods + VDF matrix, layers 2: modified $PbTiO_3$ PFC). (a) and (b), $e_{31}^*(m,n)$ for fixed $m$ values; (c), and (d), $\zeta_e^*(m,n)$ for fixed $m$ values; (e), (f), and (g), $\zeta_d^*(m,n)$ for fixed $m$ values; (f), (g), and (h), $\zeta_d^*(m,n)$ for fixed $m$ values; In all the plots, marking figures 1, 2, 3, 4, 5, 6, 7, 8, 9, and 10 correspond to volume concentrations $m = 0.01$, 0.1, 0.2, 0.3, 0.4, 0.5, 0.6, 0.7, 0.8, and 0.9, respectively.

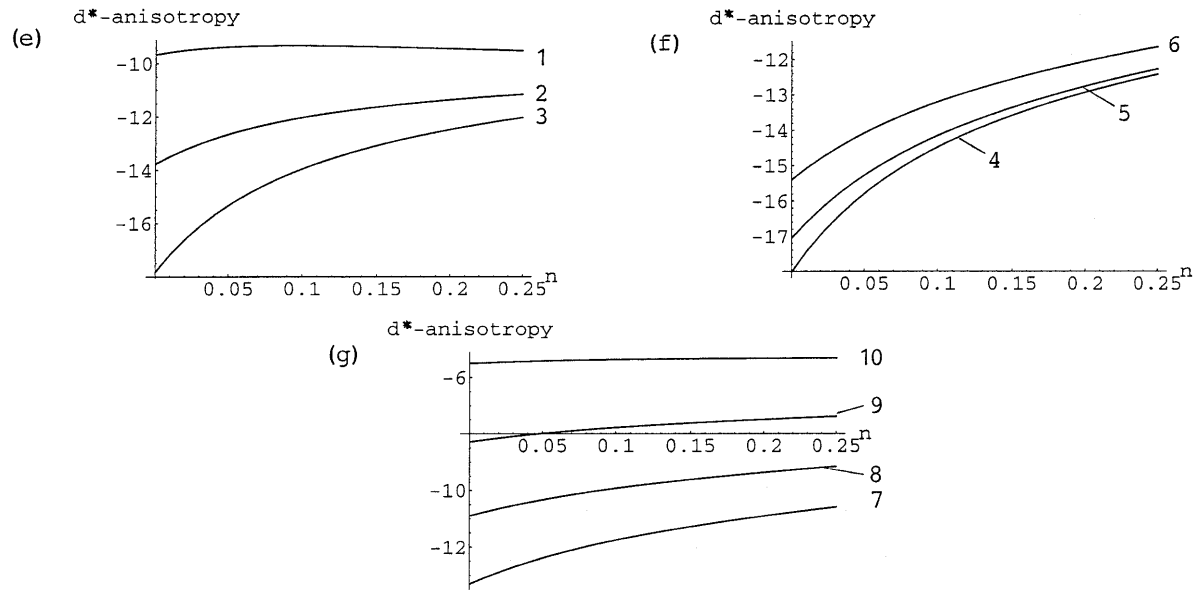


*Fig. 4.* (*Continued*)

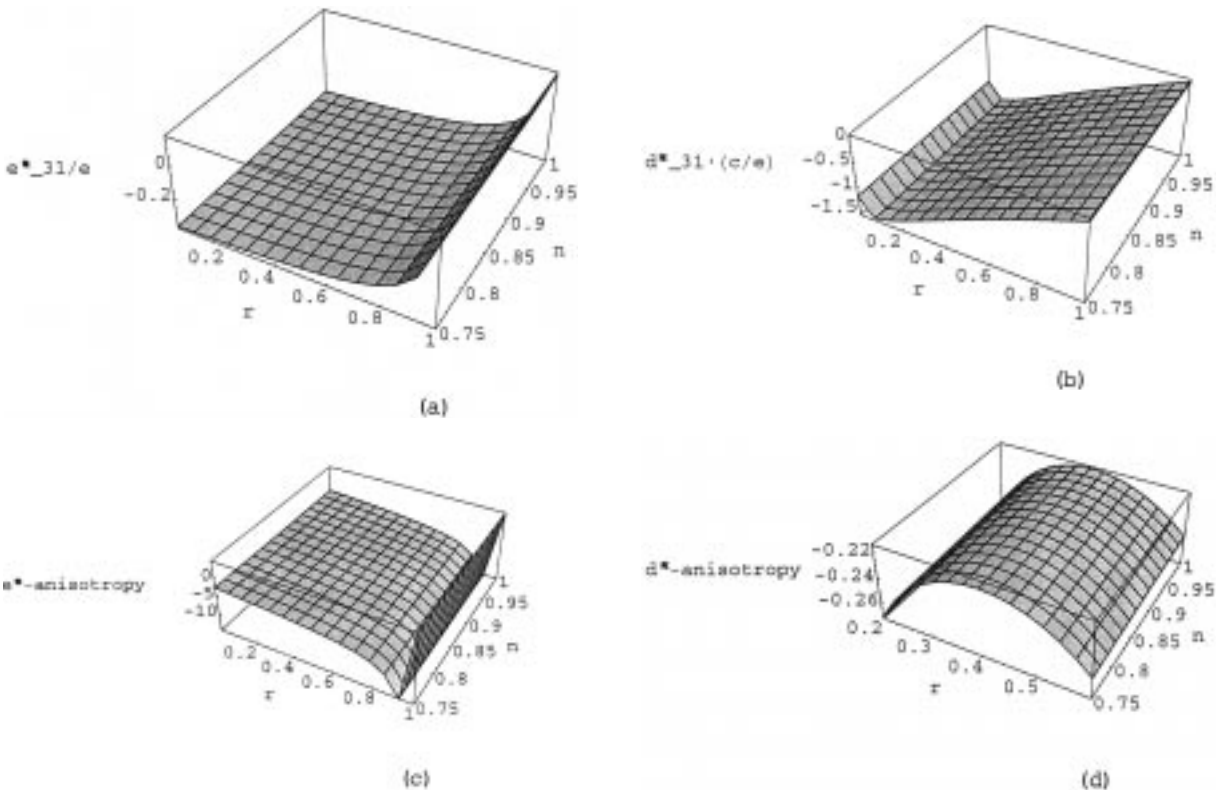


*Fig. 5.* Concentration dependences of the piezoelectric properties calculated for the composite of the type 2 with laminated rods (modified $PbTiO_3$ PFC and (Ba, Ca, Pb)$TiO_3$ PFC in layers 1 and 2, respectively) embedded in the VDF matrix. (a), $e^*_{31}(n,r)/e$; (b), $d^*_{31}(n,r)\cdot c/e$; (c), $\zeta^*_e(n,r)$; (d), (e), and (f), $\zeta^*_d(n,r)$.

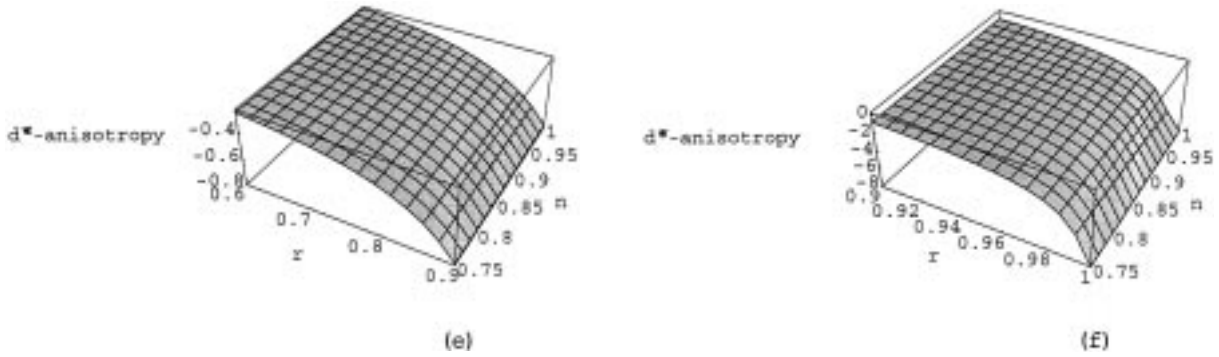


*Fig. 5.* (*Continued*)

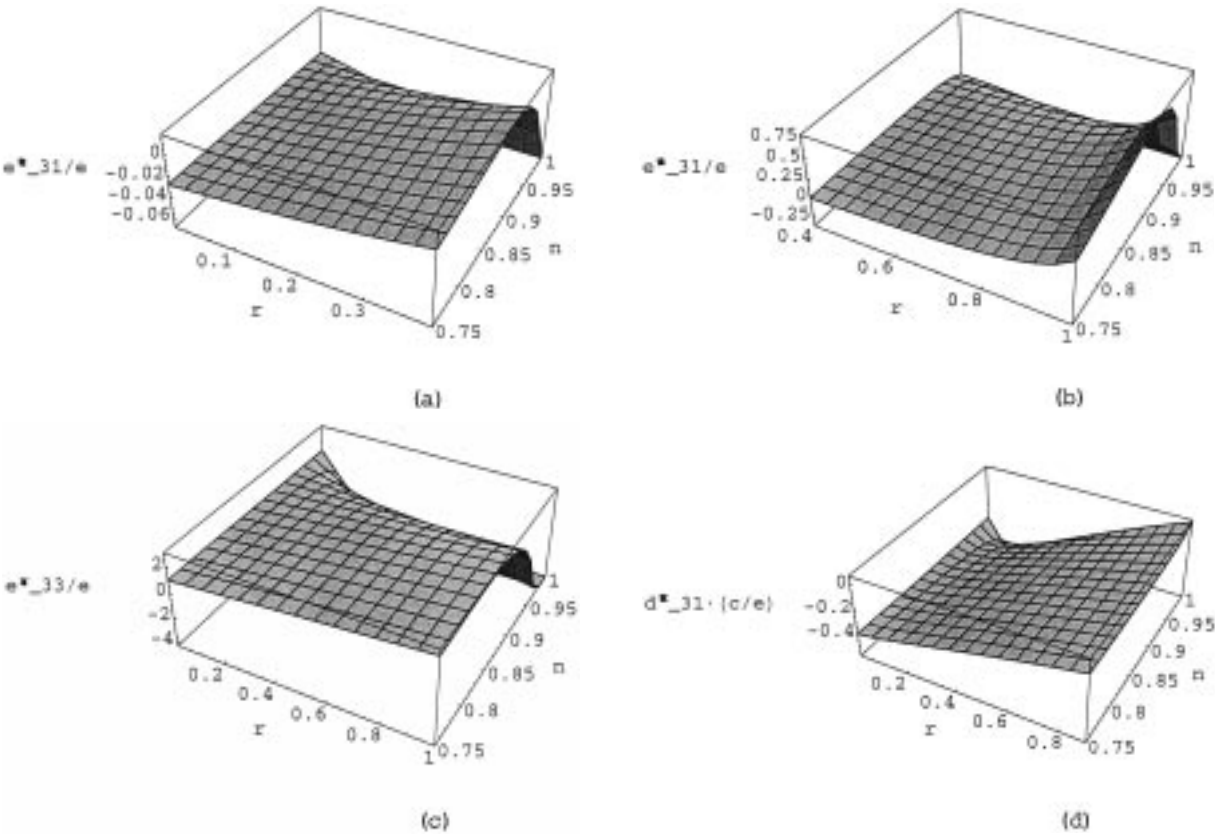


*Fig. 6.* Concentration dependences of the piezoelectric properties calculated for the composite of the type 2 with laminated rods (modified $PbTiO_3$ PFC and VDF/TrFE in layers 1 and 2, respectively) embedded in the VDF/TrFE matrix. (a) and (b), $e^*_{31}(n,r)/e$; (c), $e^*_{33}(n,r)/e$; (d) and (e), $d^*_{33}(n,r)\cdot c/e$; (g), $\zeta^*_e(n,r)$; (h) and (i), $\zeta^*_d(n,r)$.

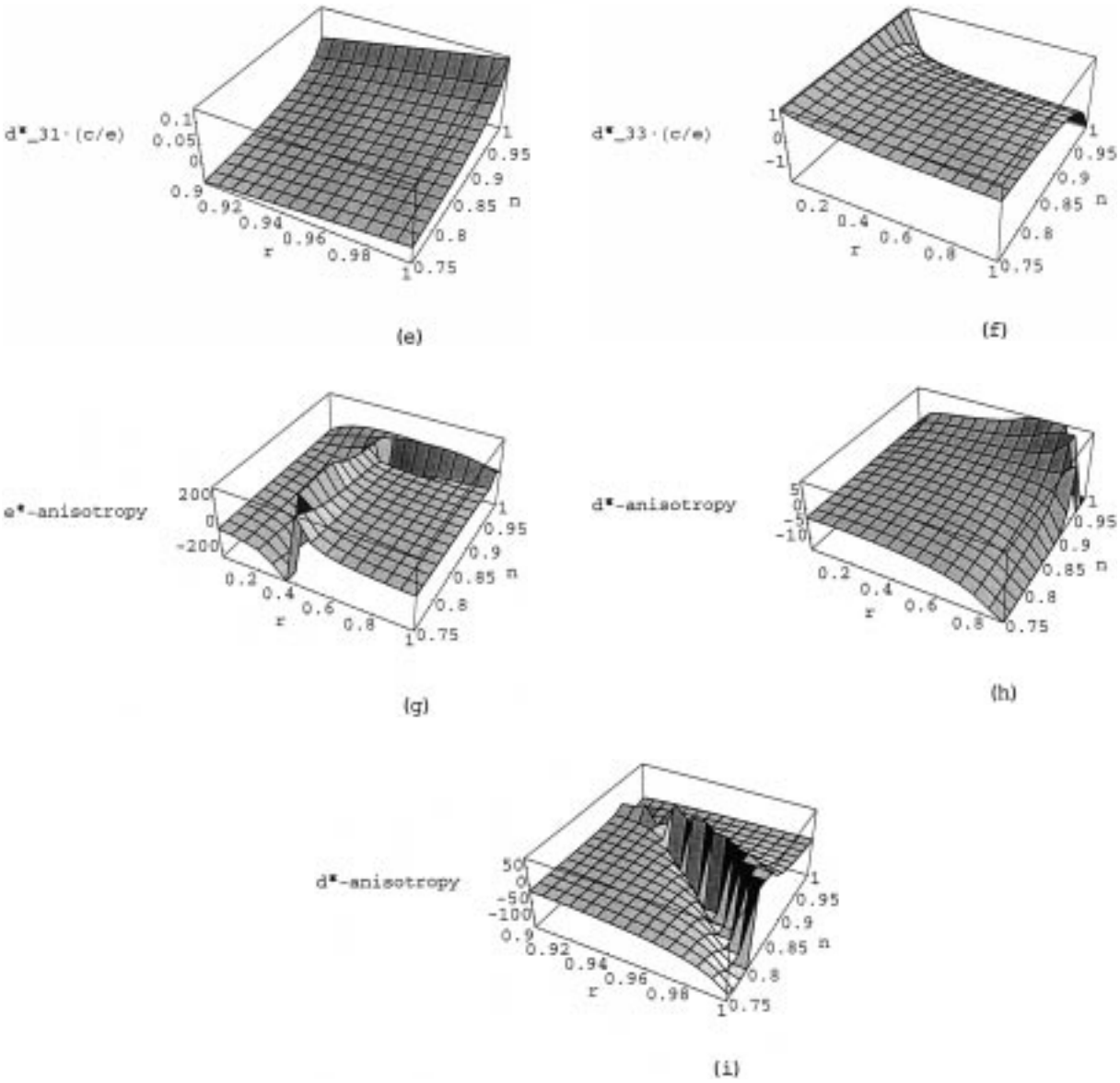


*Fig. 6.* (*Continued*)

layers within several rods along the $OX_3$ axis plays the passive role. The plots in Fig. 6(a–f ) correspond to an unusual example of all the constants $e_{31}^{(k)} > 0$ determining the piezoelectric response of the components in the $OX_1$ and $OX_2$ directions under an external electric field $\mathbf{E} \| OX_3$, and, hence, both the concentrations $n$ and $r$, describing a distribution of the components along the $OX_3$ and $OX_1$ (or $OX_2$) axes, respectively, play a remarkable role in forming the piezoelectric properties of the composite. It would be added, that even at all $e_{31}^{(k)} > 0$, one can reach $e_{31}^{*}(n, r) < 0$ within the wide $n$ and $r$ ranges, i.e., regions of the surfaces $e_{31}^{*} = e_{31}^{*}(n, r)$, where $e_{31}^{*}/e > 0$ because of $e = e_{33}^{(M)} < 0$. This circumstance is interpreted by a significant redistribution of internal stress fields within the composite sample due to the presence of the VDF/TrFE polymer as one of the layers in the rods and as the matrix surrounding these

rods (see Fig. 1(b)). In contrast to the VDF/TrFE, the $PbTiO_3$-based PFC are characterized by $e_{3j}^{(k)} > 0$ and do not influence directly changing $sgn\, e_{31}^*(n,r)$ in the composite.

Generally speaking, the different types of the $e_{3j}^*$ and $d_{3j}^*$ dependences shown in Figs. 2–6 can be plotted by using a series of fragments of stylized graphs (Fig. 7) for the piezoelectric strain $e_{3j,l}$, $e_{3j,r}$ and charge $d_{3j,l}$, $d_{3j,r}$ coefficients. These coefficients are evaluated in accordance with Eqs. (1) and (2) for the two-component ceramic/polymer 2–2 and 1–3 [19] composites, respectively. The $e_{3j,l}$ and $d_{3j,l}$ functions are considered as functions of the volume concentration $m$ of PFC layers, the $e_{3j,r}$ and $d_{3j,r}$ functions have an argument $m$ being the volume concentration of PFC rods. The constituent materials are chosen among the typical PFC and piezoactive polymers [3,18]. A further procedure supposes averaging the evaluated $e_{3j,l}$, $e_{3j,r}$, $d_{3j,l}$, and $d_{3j,r}$ coefficients with due regard for the third component and, finally, plotting the $e_{3j}^*(m,n)$ and $d_{3j}^*(m,n)$ or $e_{3j}^*(n,r)$ and $d_{3j}^*(n,r)$ dependences. However, it is obvious that such ''graphic averaging'' reflects features of the above-mentioned concentration dependences for the considered three-component composites incompletely.

One of the important reasons consists in the boundary conditions which should be carefully taken into account for the electric and mechanical fields at numerous interfaces within both the composite samples (see Fig. 1). The presence of the interfaces, having both parallel and perpendicular orientations with respect to the polarization direction ($OX_3$ axis), causes many regions, where, for example, the electric fields are concentrated within several components. An analysis of details of a possible field distribution within the entire composite sample and of its influence on the piezoelectric response of these components presents an independent problem which was not yet solved by using known analytical methods.

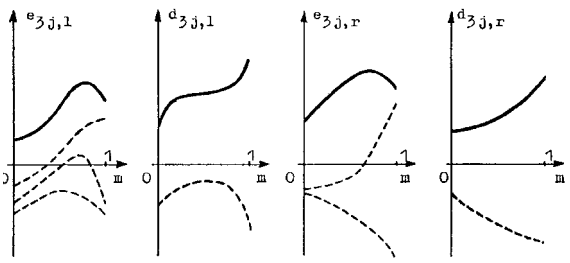


*Fig. 7.* Stylized plots of concentration dependences of piezoelectric coefficients $e_{3j,l}(m)$, $d_{3j,l}(m)$, $e_{3j,r}(n)$ and $d_{3j,r}(n)$ of two-component 2–2 (with a subscript $l$) and 1–3 (with a subscript $r$) PFC / polymer composites. Different types of dotted curves ($j = 1$) are associated with different $e_{31}^{(k)}$ and ratios between corresponding elastic moduli of chosen components, all solid curves belong to $j = 3$. For all the plots, $m$ is the volume concentration of the PFC component.

## 4. Piezoelectric Anisotropy and its Variation

Examples of various plots of the piezoelectric anisotropy $\zeta_e^* = e_{33}^*/e_{31}^*$ and $\zeta_d^* = d_{33}^*/d_{31}^*$ for the studied composites (Figs. 2–6) show how strongly these functions depend on volume concentrations and $sgn\, e_{31}^{(k)}$ of the PFC and polymer components. Several discontinuity points $\zeta_e^* \to \pm\infty$ (Figs. 2(d,e), 4(c,d), 5(c), and 6(g)) and $\zeta_d^* \to \pm\infty$ (Fig. 6(h,i)) are observed for the volume concentrations providing changes in $sgn\, e_{31}^*$ (see, e.g., Figs. 2(a,b) and 4(a, b)) and $sgn\, d_{31}^*$ (Fig. 6(d,e)). In many cases, being free of the mentioned discontinuity points, the $|\zeta_e^*(m,n)|$ and $|\zeta_e^*(n,r)|$ values become significantly more than the $e_{33}^{(k)}/|e_{31}^{(k)}|$ ratios of the chosen components listed in Table 1. This effect is realized due to an influence of the laminated structure, as shown, for example, on the $e_{31,l}(m)$ plots (Fig. 7) with $sgn\, e_{31,l}(0) = sgn e_{31,l}(1) < 0$ and $sgn\, e_{31,l}(m) > 0$ in a middle part of the $m$ range.

Plots typical of concentration dependences of the composite anisotropy for the type 1 are given in Figs. 2(f–h) and 4(e–g). As in many cases of other combinations of the PFC components, optimal volume concentrations [2] of the PFC rods $n_{opt,d}(m)$ provide $\min \zeta_d^*(m,n)$ or $\max |\zeta_d^*(m,n)|$ and have values within a range of $0.01 < n_{opt,d} < 0.1$ for various $m$ concentrations. As seen from the analysis of the calculated concentration dependences $\zeta_{m,d}^*(m) = d_{33}^*(m, n_{opt,d})/d_{31}^*(m, n_{opt,d})$ and relations between electromechanical constants [3,4,18] of the chosen components, $\max |\zeta_{m,d}^*(m)|$ points are reached for different compositions even in a presence of the non-piezoelectric araldite matrix (Table 2). Of particular interest are the cases where the modifed $PbTiO_3$ component fills the layer 2 (see the last column in Table 2) and $15 < \max |\zeta_{m,d}^*| < 20$ without a considerable dependence on the $e_{33}^{(k)}/|e_{31}^{(k)}|$ ratios for rod components (see Table 1). This fact may be interpreted if to take into consideration $sgn\, e_{3j}^{(k)}$ of the modified $PbTiO_3$ PFC and jumps of the

electromechanical constants of the components at interfaces between the layers 1 and 2 ($x_3 = \text{const}$). Such the jumps and, hence, a redistribution of the internal fields, become more appreciable for small $n_{opt,d}$ values (i.e., at a slight piezoelectric activity of the layer 1) and $m \approx 1/2$ (that provides a regular distribution of the layers of both the types along the $OX_3$ axis).

Side by side with the above-mentioned, more considerable differences in the $e_{33}^{(k)}/|e_{31}^{(k)}|$ ratios for the PFC components with $sgn e_{31}^{(k)} = -sgn\, e_{33}^{(k)} < 0\,(k = 1;2)$ promote additional increasing the $\max|\zeta_{m,d}^*(m)|$ value. As follows from Table 2, in the case of the (Pb, Ba)(Zr, Ti)$O_3$ and (Ba, Ca, Pb) $TiO_3$ PFC components this increasing can exceed 20% in comparison with the PZT-4 and ZTS-19 PFC components based on (Pb, Zr)$TiO_3$ solid solutions and having practically equal $e_{33}^{(k)}/|e_{31}^{(k)}|$ values (see Table 1). These results are in agreement with previous suppositions on the redistribution of the internal electric and mechanical fields.

Calculations based on the analysis of the electromechanical interaction of a piezoactive inclusion and a surrounding medium [20] show that the proposed composite of the type 1 provides an original distribution of induced strains $\xi_{33}^{(k)}$ along the polarization axis. So, the $|\xi_{33}^{(1)}|$ value increases considerably in the PFC rods surrounded by the less hard polymer matrix of the layer 1, and the $|\xi_{33}^{(2)}|$ value decreases in the PFC layer 2 being more hard in comparison with the layer 1. Such decreasing is also associated with an equality of the internal mechanical stresses $\sigma_{33}^{(1)} = \sigma_{33}^{(2)}$ at the interfaces ($x_3 = \text{const}$).

A more interesting and unexpected behavior of the $\zeta_d^*(n,r)$ functions for the composite type 2 is shown in Fig. 5(d–f). Within the concentration range of $0.2 < r < 0.6$ there are a vast plateau with $d_{33}^*(n,r) \to 0$ and a lack of the considerable anisotropy $\zeta_d^*$ in the system where both the PFC components are materials [3,18] with the large $d_{33}^{(k)}/|d_{31}^{(k)}|$ values. Reasons for such the behavior of the $d_{33}^*(n,r)$ functions consist in different $sgn\, e_{31}^{(k)}$ of the chosen PFC components and in $c_{33}^{(k),E}/c_{13}^{(k),E}$ (or $s_{33}^{(k),E}/s_{13}^{(k),E}$) ratios of all the three components. The piezoelectric charge coefficients of the composite are expressed according to formulas for piezoelectric media [21] as follows:

$$\left.\begin{aligned} d_{33}^* &= \frac{(c_{11}^{*E} + c_{12}^{*E})e_{33}^* - 2c_{13}^{*E}e_{31}^*}{(c_{11}^{*E} + c_{12}^{*E})c_{33}^{*E} - 2(c_{13}^{*E})^2} \\ \text{and} \qquad & \\ d_{31}^* &= \frac{c_{33}^{*E}e_{31}^* - c_{13}^{*E}e_{33}^*}{(c_{11}^{*E} + c_{12}^{*E})c_{33}^{*E} - 2(c_{13}^{*E})^2} \end{aligned}\right\} \qquad (3)$$

where $e_{3j}^*$ and $c_{fg}^{*E}$ are the effective piezoelectric strain coefficients and elastic moduli ($E = \text{const}$) of the composite, respectively. According to Eqs. (3), the $d^*-$ anisotropy factor

$$\zeta_d^* = [(c_{11}^{*E} + c_{12}^{*E})e_{33}^* - 2c_{13}^{*E}e_{31}^*]/(c_{33}^{*E}e_{31}^* - c_{13}^{*E}e_{33}^*)$$

directly depends [1] on the $e_{3j}^{(k)}$ and $c_{j3}^{(k),E}$ values or the $e_{33}^{(k)}/e_{31}^{(k)}$ and $c_{33}^{(k),E}/c_{13}^{(k),E}$ ratios which are determined for the several components. In the case of Fig. 5 the $c_{33}^{(k),E}/c_{13}^{(k),E}$ values are equal to 5.45, 2.81, and 1.31 for the modified $PbTiO_3$, (Ba, Ca, Pb)$TiO_3$ PFC's, and the VDF, respectively, and the $e_{33}^{(k)}/e_{31}^{(k)}$ ratios are also varied within a wide range covering both the negative and positive regions (see Table 1).

A presence of the VDF/TrFE components within the rods and in the matrix of the composite of the type 2 leads to increasing the $|\zeta_d^*|$ values (see Fig. 6) in spite of differences in the $c_{33}^{(k),E}/c_{13}^{(k),E}$ values being equal to 5.45 and 2.75 for the modified $PbTiO_3$ PFC and the VDF/TrFE, respectively. In this case the possibility for $d_{31}^*(n,r) = 0$ is realized at

$$n \to 1 \text{ and } r > 0.7 \qquad (4)$$

mainly due to differences in $sgn\, e_{3j}^{(k)}$ of the above-mentioned components and, additionally, the $e_{3j}^*(n,r)$ functions also pass through the zero value in the concentration ranges (4). A simple comparison of the

*Table 2.* Values of $\max|\zeta_{m,d}^*(m)| = |\zeta_{m,d}^*(m_{opt,d})|$ calculated for the composite of the type 1 containing the araldite in the layer 1

| PFC rods in the layer 1 | PZT-4 | ZTS-19 | (Pb, Ba)(Zr, Ti)$O_3$ | (Ba, Ca, Pb)$TiO_3$ | Modified $PbTiO_3$ | (Ba, Ca, Pb)$TiO_3$ | Modified $PbTiO_3$ |
|---|---|---|---|---|---|---|---|
| PFC layer 2 | ZTS-19 | PZT-4 | (Ba, Ca, Pb)$TiO_3$ | (Pb, Ba)(Zr, Ti)$O_3$ | (Ba, Ca, Pb)$TiO_3$ | (Ba, Ca, Pb)$TiO_3$ | Modified $PbTiO_3$ |
| $m_{opt,d}$ | 0.52 | 0.59 | 0.51 | 0.55 | 0.47 | 0.52 | 0.55 |
| $10^2 n_{opt,d}$ | 1.8 | 2.4 | 1.3 | 2.5 | 2.8 | 2.6 | 3.7 |
| $\max\|\zeta_{m,d}^*\|$ | 8.9 | 8.0 | 9.9 | 9.2 | 12 | 9.9 | 17 |

results from Fig. 6(a–c) with ones shown in Fig. 3(a–f) enables to observe an analogy of the $e^*_{3j}$ and $d^*_{3j}$ functions determined for both the composite types with the same components. Really, the PFC component is assumed to be distributed as inclusions of the cylindrical shape within the homogeneous polymer matrix in agreements with the conditions described in section 2. The relatively small volume concentrations $n$ of the PFC rods within the composite of the type 1 remain insufficient for changing $sgn\ e^*_{31}(m,n)$ even at values of $e^*_{31} \sim 10^{-3}\mathrm{C/m}^2$ (see Fig. 3(a–c)) whereas the condition $e^*_{33}(m,n) = 0$ is fulfilled (Fig. 3(f)). The plots in Fig. 6(a,b) and Fig. 6(c) show the analogous trends for the $e^*_{31}(n,r)$ and $e^*_{33}(n,r)$ functions, respectively, which have been determined for the composite of the type 2, and indicate the above-mentioned common factors determining the large piezoelectric anisotropy in both the structures.

## 5. Summary

The proposed results of modeling and comparative study of the composites with variable connectivity show the role of $sgn\, e^{(k)}_{3j}$ of the chosen components and the distribution of internal electric and elastic fields within the composites in forming their piezoelectric properties. Such the factors as microgeometry, the piezoelectric anisotropy of the several components, and differences in the analogous electromechanical constants of the components distinctly influence the $\zeta^*_e$ and $\zeta^*_d$ values. The variable connectivity factor being taken into consideration enables to reach significant jumps of some components of vectors (tensors) of the internal electric and elastic fields and, therefore, to influence the piezoelectric anisotropy of the composite sample as a whole. Thus, variable connectivity can play the prominent role of the link between the anisotropy of the electromechanical properties of several components and the anisotropy of the analogous properties of the studied composite structures. Finally, it seems to be interesting and important to create the composite materials with the $\zeta^*_e$ and $\zeta^*_d$ dependences analogous to shown in Figs. 2(d,e), 3(g–i), 4(c,d), 5(c), 6(g) and Figs. 5(d–f), 6(h,i), respectively, and to use these materials for different applications. The undertaken study can also promote a selection of ferro- or piezoelectric ceramic components for a creation of novel composite materials with the piezoelectric properties being high-anisotropic (i.e., $|\zeta^*_e| > 10$ or $|\zeta^*_d| > 10$) or varied within wide ranges.

## Acknowledgment

The authors would like to thank Prof. Dr. G. Arlt and Prof. Dr. R. Waser (RWTH Aachen, Germany) for interest in the research and helpful discussions. Financial support by the Deutsche Forschungsgemeinschaft (Germany) during the stay by one of the authors (V.Yu.T.) at the RWTH Aachen is also acknowledged.

## References

1. A.V. Turik and V.Yu. Topolov, *J. Phys. D: Appl. Phys.*, **30**, 1541 (1997).
2. V.Yu. Topolov and A.V. Turik, *Piss'ma ZhTF*, **24**(11), 65 (1998, in Russian); *Tech. Phys. Lett.*, **24**, 441 (1998).
3. L.P. Khoroshun, B.P. Maslov, and P.V. Leshchenko, *Prognostication of Effective Properties of Piezoactive Composite Materials* (Naukova Dumka, Kiev, 1989), p. 208 (in Russian).
4. H.L.W. Chan and J. Unsworth, *IEEE Trans. Ultrason., Ferroelec., a. Freq. Contr.*, **36**, 434 (1989).
5. J. Bennett and G. Hayward, *IEEE Trans. Ultrason., Ferroelec., a. Freq. Contr.*, **44**, 565 (1997).
6. O. Sigmund, S. Torquato, and I.A. Aksay, *J. Mater. Res.*, **13**, 1038 (1998).
7. W. Cao, Q.M. Zhang, and L.E. Cross, *IEEE Trans. Ultrason., Ferroelec., a. Freq. Contr.*, **40**, 103 (1993).
8. H. Taunaumang, I.L. Guy, and H.L.W. Chan, *J. Appl. Phys.*, **76**, 484 (1994).
9. L. Li and N.R. Sottos, *J. Appl. Phys.*, **77**, 4595 (1995).
10. A.A. Grekov, S.O. Kramarov, and A.A. Kuprienko, *Mekhanika Kompositnykh Materialov*, N° **1**, 62 (1989, in Russian).
11. M.L. Dunn, *J. Appl. Phys.*, **73**, 5131 (1993).
12. C.-W. Nan, *J. Appl. Phys.*, **76**, 1155 (1994).
13. F. Levassort, M. Lethiecq, D. Certon, and F. Patat, *IEEE Trans. Ultrason., Ferroelec., a. Freq. Contr.*, **44**, 445 (1997).
14. F. Levassort, M. Lethiecq, C. Millar, and L. Pourcelot, *IEEE Trans. Ultrason., Ferroelec., a. Freq. Contr.*, **45**, (1497) (1998).
15. G. Hayward and J. Bennett, *IEEE Trans. Ultrason., Ferroelec., a. Freq. Contr.*, **43**, 98 (1996).
16. A.-C. Hladky-Hennion and J.-N. Decarpigny, *J. Acoust. Soc. Amer.*, **94**, 621 (1993).
17. E. Akcakaya and G.W. Farnell, *J. Appl. Phys.*, **64**, 4469 (1988).
18. Landolt-Börnstein, *Zahlenwerte und Funktionen aus Naturwissenschaften und Technik. Neue Serie. Gr.III, Bd.18* (Springer-Verlag, Berlin, 1984), 559 pp.; Gr. III, Bd.28 (Springer-Verlag, Berlin, 1990), 833 pp.
19. V.Yu. Topolov and A.V. Turik, *J. Appl. Phys.*, **85**, 372 (1999).
20. M.L. Dunn and M. Taya, *Trans. ASME: J. Appl. Mech.*, **61**, 474 (1994).
21. *Keramik*, edited by H. Schaumburg (Teubner, Stuttgart, 1994), p. 650.